Effect of Bulkiness of Pendent Side Groups on the Rheology of Semiflexible Main-Chain Thermotropic Liquid-Crystalline Polymers

Dong-Ok Kim and Chang Dae Han*

Department of Polymer Engineering, The University of Akron, Akron, Ohio 44325

Received September 17, 1999

ABSTRACT: The effect of bulkiness of pendent side groups on the rheology of semiflexible main-chain thermotropic liquid-crystalline polymers (TLCPs) was investigated. The TLCPs investigated have aromatic triads with 10 methylene groups as flexible spacer and varying pendent side groups: ethoxy group, *tert*-butyl group, and phenylsulfonyl group. The TLCP having ethoxy pendent side groups (PEHQ10) undergoes smectic−nematic transition at 148 °C and nematic−isotropic (N−I) transition at 239 °C, the TLCP having *tert*-butyl pendent side groups (PTHQ10) undergoes only N−I transition at 193 °C, and the TLCP having phenylsulfonyl pendent side groups (PSHQ10) undergoes only N−I transition at 179 °C. Comparison of the rheological behavior of the three TLCPs was made at 40 °C below the N−I transition temperature (T_{NI}) and at 15 °C above the T_{NI}. The following observations were made. Upon startup of shear flow all three TLCPs exhibited a large overshoot in shear stress (σ) followed by monotonic decay and a very large overshoot in first normal stress difference (N_1) followed by oscillatory decay. The peak values of overshoot in both σ and N_1 increased with increasing bulkiness of pendent side groups, and only *positive* N_1 was observed over the entire range of shear rates and temperatures investigated. Upon cessation of steady-state shear flow the relaxation rate of both σ and N_1 decreased with increasing bulkiness of pendent side groups, and during rest after cessation of steady-state shear flow the rate of increase in *reduced* dynamic loss modulus was fastest in PTHQ10 and slowest in PSHQ10. In the nematic state the differences in bulkiness of pendent side groups played an important role, while in the isotropic state the differences in molecular weight played an important role in determining the viscosities of the TLCPs.

1. Introduction

In the past, numerous papers have been published reporting on the rheological behavior of thermotropic liquid-crystalline polymers (TLCPs) having a clearing temperature *higher* than the thermal degradation temperature. There are too many papers to cite them all here, and the readers are referred to a few selected papers and references therein.[1,2] However, use of such TLCPs for rheological investigation poses a serious problem with obtaining reproducible results, owing to a practical difficulty with establishing reproducible initial conditions (i.e., reproducible initial morphological state prior to rheological measurement).[3] This is because the morphological state of a TLCP is very sensitive to previous thermal history; thus, different thermal history of a TLCP specimen prior to rheological measurement may give rise to different rheological responses.[3−5] Some investigators[6] claimed that preshearing a TLCP specimen in an anisotropic state enabled them to stabilize its morphological state, thus providing reproducible initial conditions. On the other hand, the duration of preshearing also affects the initial morphological state of a specimen prior to rheological measurement, as demonstrated by Han et al.[3] The origin in the difficulty of controlling initial conditions of a TLCP lies in that, during rheological measurement, the polymer may undergo crystallization[4,7] and/or the mesophase may grow continuously even when the polymer is noncrystallizable.[8]

The most effective way of circumventing the difficulty described above is to erase previous thermal and deformation histories by heating a specimen above its clearing temperature for a sufficiently long period before cooling down to a preset temperature in an anisotropic state, at which rheological measurements are to be taken. Such procedure is only possible when TLCPs having a clearing temperature *below* thermal degradation temperature are available. Han and co-workers[3−5,9−11] indeed successfully adopted such a procedure after having synthesized TLCPs having clearing temperatures *far below* their thermal degradation temperatures.

Needless to say, the rheological behavior of TLCPs would depend on their chemical structures. At present we do not have a comprehensive theory that enables us to generalize the rheological behavior of TLCPs in terms of the chemical structure of TLCP. To date there are relatively few experimental studies reported in the literature describing the effect of chemical structure of TLCPs on their rheological behavior. There are a very large number of chemical structures that give rise to liquid crystallinity in polymer, and thus it is virtually impossible to take rheological measurements for all those TLCPs synthesized so far.

Lenz and co-workers[12,13] were the first to demonstrate that the presence of pendent side groups in a main-chain TLCP decreases both melting point and clearing temperature. Following their studies, Han and co-workers[5,9,14] synthesized a homologous series of TLCPs having the chemical structure

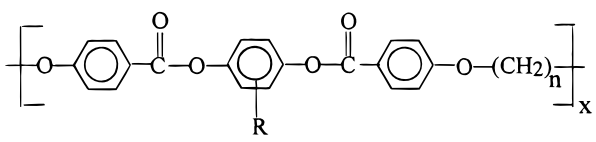

I

with R = SO_2-Ph and n = 3−12, and investigated their rheological behavior.[3−5,9−11]

As part of our continuing efforts to enhance our understanding of the rheological behavior of TLCPs, very recently we synthesized polymer **I** with n = 10 and

10.1021/ma9915879 CCC: $19.00
Published on Web 04/12/2000

Table 1. Summary of the Intrinsic Viscosity of the TLCPs Investigated and van der Waals Volume of Pendent Side Groups in the TLCPs

sample code	[η] (dL/g) at 23 °C[a]	van der Waals vol of pendent side group (nm^3)[b]
PEHQ10	1.393	54.0×10^{-3}
PTHQ10	0.771	82.7×10^{-3}
PSHQ10	0.667	121.0×10^{-3}

[a] Each polymer sample was first dissolved in 1,1,2,2-tetrachloroethane at an elevated temperature and then cooled to room temperature for [η] measurement at 23 °C. [b] Calculated using the Cerius[2] program of molecular simulations software.

pendent side groups R = OC_2H_5, $C(CH_3)_3$, or SO_2-Ph.[15] In this study, we investigated their rheological behaviors, putting emphasis on the effect of bulkiness of pendent side groups. In this paper we report the highlights of our findings.

2. Experimental Section

2.1. Materials. We synthesized by either melt or solution polycondensation reactions of monomer **II** with $n = 10$ and monomer **III** having pendent side groups, R = OC_2H_5, $C(CH_3)_3$, or SO_2-Ph, yielding

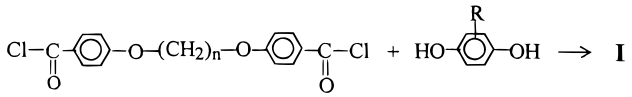

II **III**

Below polymer **I** with $n = 10$ and OC_2H_5 pendent side groups will be referred to as PEHQ10, polymer **I** with $n = 10$ and $C(CH_3)_3$ pendent side groups will be referred to as PTHQ10, and polymer **I** with $n = 10$ and SO_2-Ph pendent side groups will be referred to as PSHQ10. The details of the synthesis procedures for monomer **II** are described elsewhere.[5,12] Monomer **III** was either purchased or prepared in our laboratory. Following the procedure described by Lenz et al.,[13] ethoxyhydroquinone for the synthesis of PEHQ10 was prepared from 3-ethoxy-4-hydroxybenzaldehyde, which was purchased from Aldrich. Following the procedures described in the literature,[5,12] 2-phenylsulfonyl-1,4-hydroquinone for the synthesis of PSHQ10 was prepared. *tert*-Butylhydroquinone for the synthesis of PTHQ10 was purchased from Aldrich. The details of the polycondensation reactions are described elsewhere.[5,12] In a separate study[15] we found via wide-angle X-ray diffraction and polarized optical microscopy that PEHQ10 forms smectic and nematic mesophases while PTHQ10 and PSHQ10 form only nematic mesophase, indicating that the molecular packing in PEHQ10 is much greater than that in PTHQ10 and PSHQ10. We measured the intrinsic viscosities [η] of the three TLCPs using an Ubbelohde viscometer. Table 1 gives a summary of [η] for the three TLCPs employed in this study. In view of the fact that [η] increases with increasing molecular weight, below we will use the information on [η] given in Table 1 to interpret the effect of molecular weight of the TLCPs investigated on their rheological responses observed in this study.

2.2. Rheological Measurement. For rheological measurements, specimens with a thickness of 0.5 mm were prepared by solvent casting from dichloromethane in the presence of 0.1 wt % antioxidant (Irganox 1010, Ciba-Geigy Group) and then slowly evaporating the majority of the solvent first at room temperature for 1 week and then at a temperature 10 °C *below* the glass transition temperature (T_g) for 3 days in a vacuum oven to remove any residual solvent. Specimens were dried further in a vacuum oven at a temperature 10 °C *above* the T_g of each polymer for 2 h. From our previous study[15] we had information on the T_g of each polymer: (i) PEHQ10 has $T_g = 51$ °C, (ii) PTHQ10 has $T_g = 67$ °C, and (iii) PSHQ10 has $T_g = 84$ °C. A Rheometrics mechanical spectrometer (RMS model 800) with a cone-and-plate (8 mm diameter plate, 0.1 rad cone angle) fixture was used to measure the following: (1) in the transient shear mode, shear stress growth ($\sigma^+(t,\dot{\gamma})$) and first normal stress difference growth ($N_1^+(t,\dot{\gamma})$) as functions of time (t) for various shear rates ($\dot{\gamma}$) and temperatures, and (2) in the steady-state shear mode, shear stress (σ), shear viscosity (η), and first normal stress difference (N_1) as functions of shear rate ($\dot{\gamma}$) and temperature. Using a parallel-plate (8 mm diameter) fixture, the dynamic storage modulus (G') and dynamic loss modulus (G'') were measured as functions of angular frequency (ω), for which strain amplitude was varied from 0.01 to 0.06, which was well within the linear viscoelastic range of the materials investigated. All experiments were conducted under a nitrogen atmosphere in order to preclude oxidative degradation of the specimen. The temperature control was satisfactory to within ±1 °C.

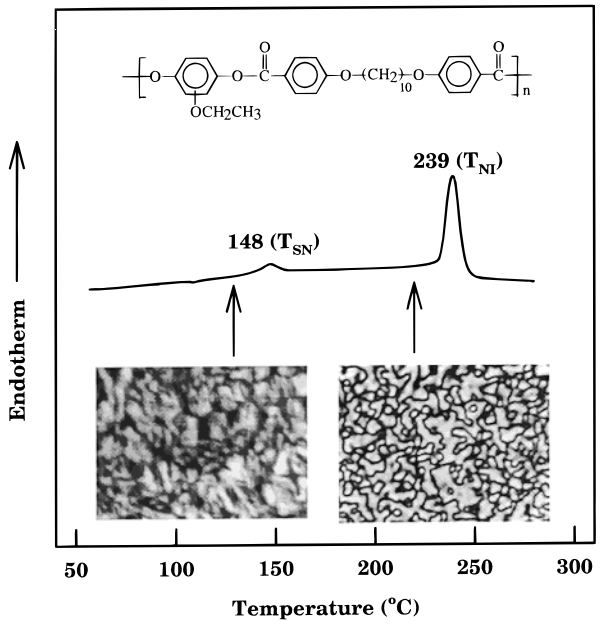

Figure 1. DSC trace and polarizing optical micrograph of PEHQ10.

3. Results and Discussion

Before presenting the rheological behavior of the three TLCPs under investigation, we first present the thermal transitions and mesophase structures of these polymers. We believe that such information is necessary for the readers to understand how the rheological behavior of each polymer is affected by the mesophase structure in an anisotropic state at different temperatures. Moreover, such information will facilitate the discussion of the rheological measurements taken in this study.

Figure 1 gives a differential scanning calorimetry (DSC) trace for PEHQ10, showing that this polymer has a smectic−nematic (S−N) transition temperature (T_{SN}) of 148 °C and a nematic−isotropic (N−I) transition temperature (T_{NI}) of 239 °C. This observation is in good agreement with that reported in a paper by Hudson et al.[16] Also given in Figure 1 are two polarized optical micrographs of PEHQ10: one taken at 130 °C in the smectic region and the other taken at 220 °C in the nematic region. We had to anneal an as-cast specimen for a very long time in order to observe a distinct smectic texture. We found from DSC that PTHQ10 having *tert*-butyl pendent side groups undergoes only N−I transition at 193 °C and the PSHQ10 having phenylsulfonyl pendent side groups undergoes only N−I transition at 179 °C.[15] The information on thermal transition tem-

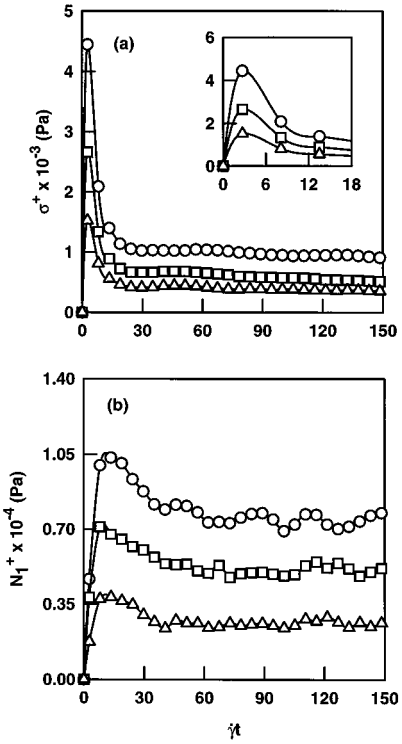

Figure 2. Plots of (a) $\sigma^+(t,\dot{\gamma})$ versus $\dot{\gamma}t$ and (b) $N_1^+(t,\dot{\gamma})$ versus $\dot{\gamma}t$, describing the growth of stresses, for PTHQ10 at $\dot{\gamma} = 0.3$ s^{-1} and at various temperatures in the nematic region: (○) 150 °C, (□) 160 °C, and (△) 170 °C.

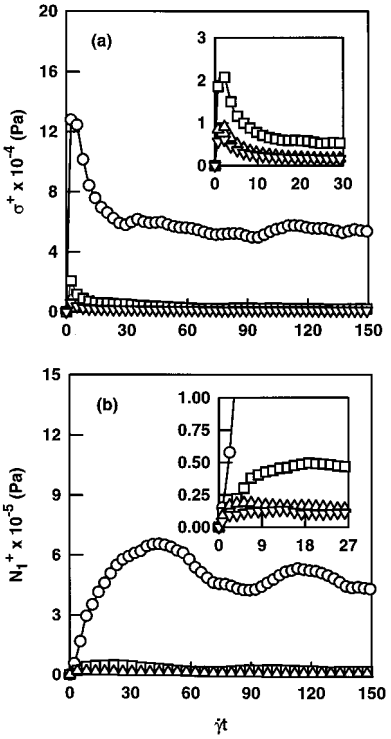

Figure 3. Plots of (a) $\sigma^+(t,\dot{\gamma})$ versus $\dot{\gamma}t$ and (b) $N_1^+(t,\dot{\gamma})$ versus $\dot{\gamma}t$, describing the growth of stresses, for PEHQ10 at $\dot{\gamma} = 0.3$ s^{-1} and at various temperatures. In the smectic region at various temperatures: (○) 135 °C. In the nematic region at various temperatures: (□) 160 °C, (△) 180 °C, and (▽) 200 °C.

peratures guided us to judiciously choose temperatures at which rheological measurements were to be taken.

Any rheological measurement of a TLCP under the influence of thermal history is of little physical significance. In the present study before commencing rheological experiments, previous thermal history of a specimen was erased by using the following temperature protocol.[3−5,9−11] First a specimen was placed in the cone-and-plate fixture that was preheated at a temperature 10 °C above the T_{NI} of each polymer specimen. An independent study indicated that decomposition of the TLCPs under investigation started at about 350 °C, which is far above the T_{NI} of the TLCPs. After the temperature of the specimen is equilibrated in the isotropic region, the specimen was sheared at $\dot{\gamma} = 0.1$ s^{-1} for about 10 min and then cooled slowly to a predetermined temperature in the nematic region, and finally the specimen was allowed to reach thermal equilibrium for about 10 min. This procedure resulted in a reproducible initial conditions (i.e., reproducible morphological state of the specimen). The same procedure was followed for all rheological experiments performed in this study. It should be emphasized that the primary purpose of the present study was to investigate the effect of bulkiness of pendent side groups on the rheological behavior of PEHQ10, PTHQ10, and PSHQ10.

3.1. Transient Shear Flow in an Anisotropic State. Figure 2 describes variations of shear stress growth $\sigma^+(t,\dot{\gamma})$ and first normal stress difference growth $N_1^+(t,\dot{\gamma})$ with strain ($\dot{\gamma}t$), upon starting a sudden shear flow, of PTHQ10 at 150, 160, and 170 °C for $\dot{\gamma} = 0.3$ s^{-1}. On the basis of our previous studies,[3−5,9−11] a fresh specimen was employed for each temperature. It can be seen in Figure 2 that upon startup of shear flow at 150 °C $\sigma^+(t,\dot{\gamma})$ goes through a maximum in a very short time, whereas $N_1^+(t,\dot{\gamma})$ goes through a maximum at $\dot{\gamma}t \approx 15$ and then undergoes an oscillation before reaching a steady-state value. However, at 170 °C the oscillation of $N_1^+(t,\dot{\gamma})$ virtually disappears. Note in Figure 2 that not only the peak values of $\sigma^+(t,\dot{\gamma})$ and $N_1^+(t,\dot{\gamma})$ but also steady-state values of $\sigma(\dot{\gamma})$ and $N_1(\dot{\gamma})$ increase as the temperature decreases (i.e., as the system moves away from T_{NI}). Similar results were obtained, not presented here, for PSHQ10.

Figure 3 describes variations of $\sigma^+(t,\dot{\gamma})$ and $N_1^+(t,\dot{\gamma})$ with $\dot{\gamma}t$, upon starting a sudden shear flow, of PEHQ10 at 135, 160, 180, and 200 °C for $\dot{\gamma} = 0.3$ s^{-1}. Note that a fresh specimen was employed for each temperature. Notice in Figure 3 that upon starting a sudden shear flow $N_1^+(t,\dot{\gamma})$ at 135 °C grows very slowly, having a peak value at $\dot{\gamma}t \approx 45$, and shows an oscillation with a large amplitude compared to $\sigma^+(t,\dot{\gamma})$. The size of the second peak in $N_1^+(t,\dot{\gamma})$ at 135 °C is indeed very large compared to that at 160 °C. Of particular interest in Figure 3 is that peak values of both $\sigma^+(t,\dot{\gamma})$ and $N_1^+(t,\dot{\gamma})$ at 135 °C in the smectic region are several times greater than those at 160 °C in the nematic region. This large difference in the peak values of $\sigma^+(t,\dot{\gamma})$ and $N_1^+(t,\dot{\gamma})$ is believed to be not due to the difference in measurement temperature alone, but due to large difference in domain texture between 2-dimensional smectic phase and 1-dimensional nematic phase. To the best of our knowledge, we are not aware of any previous study reporting on the transient shear flow behavior of a smectic TLCP.

It should be mentioned at this juncture that a study of Marrucci and Maffettone[17] predicts the appearance of multiple overshoots in $N_1^+(t,\dot{\gamma})$ during transient shear flow. But their study is based on a monodomain model that predicts a tumbling behavior and is also based on the Maier−Saupe intermolecular potential (excluded-volume interactions).[18] We are not aware of any theo-

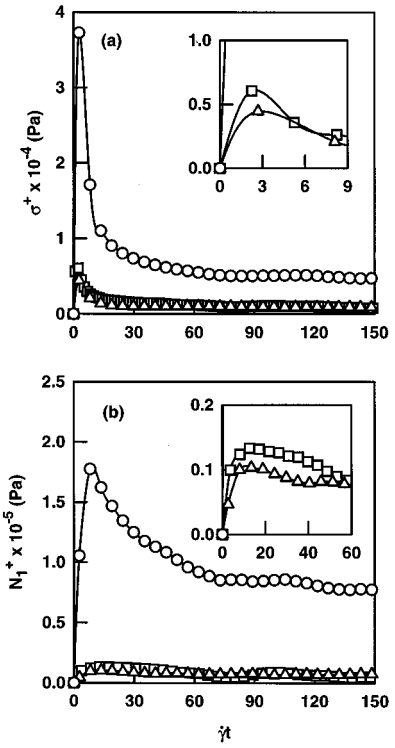

Figure 4. Plots of (a) $\sigma^+(t,\dot{\gamma})$ versus $\dot{\gamma}t$ and (b) $N_1^+(t,\dot{\gamma})$ versus $\dot{\gamma}t$, describing the growth of stresses, at $\dot{\gamma} = 0.3$ s^{-1} and at T_{NI} − 40 °C in the nematic region for (○) PSHQ10, (□) PEHQ10, and (△) PTHQ10.

retical attempt made to predict transient shear flow of segmented TLCPs with or without pendent side groups. Undoubtedly, the partial flexibility of the segmented TLCP chains would play an important role in determining transient shear flow behavior. Nevertheless, the theory of Marrucci and Maffettone appears to capture the basic features of transient shear flow behavior of TLCP.

Since the TLCPs under investigation have different molecular weights and different pendent side groups, a comparison of transient shear flow behavior among the three polymers at the same temperature would not be meaningful. Thus, we need to choose an appropriate variable(s) that might minimize the effect of molecular weight on the rheological behavior in an anisotropic state. This is because the rheological behavior of a TLCP in an anisotropic depends on how far away the experimental temperature is from the clearing temperature of the polymer. In this regard, following a previous study of Chang and Han,[11] below we will compare transient shear flow behavior of the three TLCPs under investigation at a temperature having the same distance below the T_{NI} of the respective polymers. The rationale behind this approach lies in that the T_{NI} of a TLCP becomes independent of molecular weight above a critical molecular weight.[19−23]

Figure 4 describes variations of $\sigma^+(t,\dot{\gamma})$ and $N_1^+(t,\dot{\gamma})$ with $\dot{\gamma}t$, upon initiation of a sudden shear flow, at T_{NI} − 40 °C in the nematic region for PTHQ10, PSHQ10, and PEHQ10 at $\dot{\gamma} = 0.3$ s^{-1}. In Figure 4 we observe that the peak values of $\sigma^+(t,\dot{\gamma})$ and $N_1^+(t,\dot{\gamma})$ for PSHQ10 are 8−10 times greater than those for PEHQ10 and PTHQ10. In a separate study,[15] using the Cerius^2 program of molecular simulations software (Molecular Simulations Inc.), we calculated the van der Waals volumes of the three pendent side groups, and they are summarized in Table 1. It can be seen in Table 1 that the van der Waals volumes are ranked as follows: 0.1205 nm^3 for SO_2-Ph group > 0.0827 nm^3 for $C(CH_3)_3$ group > 0.0540 nm^3 for OC_2H_5 group. Notice in Table 1 that the intrinsic viscosity of PEHQ10 is much higher than that of PSHQ10, indicating that the molecular weight of PEHQ10 is much higher than that of PSHQ10. Since our previous study[9] indicated $\eta_0 \propto M^6$ with η_0 being zero-shear viscosity and M being molecular weight and $N_1 \propto M^{6.5}$ with N_1 being first normal stress difference, we would expect to observe much larger peak values of $\sigma^+(t,\dot{\gamma})$ and $N_1^+(t,\dot{\gamma})$ for PEHQ10 than for PSHQ10, if the molecular weight played a predominant role over the bulkiness of pendent side groups. However, our experimental results given in Figure 4 show that the peak values of $\sigma^+(t,\dot{\gamma})$ and $N_1^+(t,\dot{\gamma})$ for PSHQ10 are much greater than those for PEHQ10. The above observations lead us to conclude that the difference in bulkiness between the SO_2-Ph group and OC_2H_5 group apparently outweighed the difference in molecular weight between PSHQ10 and PEHQ10 in determining the peak values of $\sigma^+(t,\dot{\gamma})$ and $N_1^+(t,\dot{\gamma})$ of the two polymers.

We would like to point out that over the entire range of shear rates and temperatures tested we only observed *positive* values of first normal stress difference during both transient shear flow ($N_1^+(t,\dot{\gamma})$) and steady-state shear flow ($N_1(\dot{\gamma})$), in agreement with previous studies.[1,3,9,10,24] Such observations are at variance with some earlier studies[25−28] on lyotropic liquid-crystalline polymers, reporting *negative* values of $N_1(\dot{\gamma})$ over a certain range of $\dot{\gamma}$. At present the origin of the observed difference in the sign of $N_1(\dot{\gamma})$ between thermotropic and lyotropic LCPs during steady-state shear flow is not well understood although some speculations were made by Baek et al.[24]

As pointed out by Han et al.,[3] an erroneous conclusion can be drawn on the sign of first normal stress difference in TLCP if transient or steady-state shear flow experiments are carried out in the presence of residual normal force that were generated during the squeezing of the specimen in an anisotropic state.[2] The residual normal force in the specimen can be made to relax completely if one waits for a very long time after a specimen is loaded on the cone-and-plate fixture of a rheometer.[3] However, by the time the residual normal force in the specimen relaxes completely, the polymer will no longer have the same morphological state because the morphological state of a TLCP in an anisotropic state depends very much on both thermal and deformation histories.[3] The only way to circumvent this difficulty, as demonstrated in Figure 5, is to first load a specimen in the cone-and-plate fixture of a rheometer at a temperature above the clearing temperature of the specimen, wait until $N_1^+(t,\dot{\gamma})$ becomes zero at rest, and then decrease the temperature very slowly stepwise, ascertaining that $N_1^+(t,\dot{\gamma})$ returns to the baseline at each temperature. Notice in Figure 5 that upon decreasing the temperature, say 5 °C, instantly $N_1^+(t,\dot{\gamma})$ increases and then decreases to a *negative* value because the gap opening between the cone and the plate must be adjusted accordingly, to keep the gap opening constant, but $N_1^+(t,\dot{\gamma})$ returns slowly to the baseline after waiting for a while. Such a procedure is essential in order to obtain reproducible initial conditions and reliable measurements of $N_1^+(t,\dot{\gamma})$ and $N_1(\dot{\gamma})$ in TLCPs in general. Needless to say, such a procedure cannot be adopted if

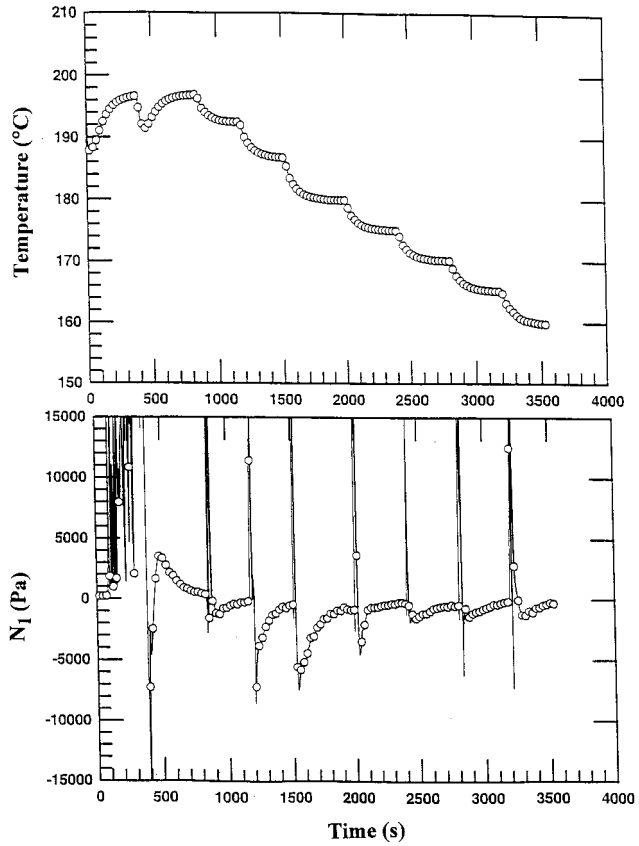

Figure 5. Temperature protocols (upper panel) and variations of first normal stress difference N_1 (lower panel) with time during the loading of PSHQ10 specimen at 195 °C in the isotropic region followed by subsequent stepwise cooling with a temperature interval of 5 °C down to 160 °C in the nematic region. The clearing temperature of PSHQ10 is 179 °C. Note that N_1 returns to the baseline (zero value) after a step change of temperature.

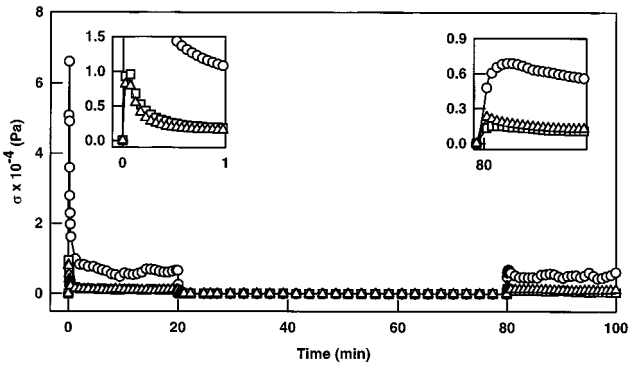

Figure 6. (a) Shear stress buildup $\sigma^+(t,\dot\gamma)$ during startup shear flow at $\dot\gamma = 0.6\ s^{-1}$, (b) stress decay $\sigma^-(t,\dot\gamma)$ upon cessation of steady-state shear flow at $\dot\gamma = 0.6\ s^{-1}$, and (c) shear stress buildup $\sigma^+(t,\dot\gamma)$ during intermittent shear flow at $\dot\gamma = 0.6\ s^{-1}$ after a rest for 60 min after cessation of steady-state shear flow at $T_{NI} - 40$ °C in the nematic region for (○) PSHQ10, (□) PEHQ10, and (△) PTHQ10.

TLCP has a clearing temperature higher than the thermal degradation temperature (e.g., Vectra A900).[1,2]

3.2. Stress Relaxation after Cessation of Shear Flow and Intermittent Shear Flow. Figure 6 describes (i) variations of $\sigma^+(t,\dot\gamma)$ upon startup shear flow, (ii) variations of shear stress decay $\sigma^-(t,\dot\gamma)$ upon cessation of steady-state shear flow, and (iii) variations of $\sigma^+(t,\dot\gamma)$ in intermittent shear flow followed by a long rest

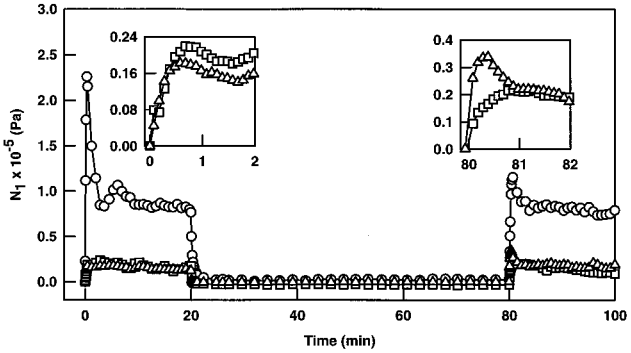

Figure 7. (a) First normal stress difference buildup $N_1^+(t,\dot\gamma)$ during startup shear flow at $\dot\gamma = 0.6\ s^{-1}$, (b) first normal stress difference decay $N_1^-(t,\dot\gamma)$ upon cessation of steady-state shear flow at $\dot\gamma = 0.6\ s^{-1}$, and (c) first normal stress difference buildup $N_1^+(t,\dot\gamma)$ during intermittent shear flow at $\dot\gamma = 0.6\ s^{-1}$ after a rest for 60 min after cessation of steady-state shear flow at $T_{NI} - 40$ °C in the nematic region for (○) PSHQ10, (□) PEHQ10, and (△) PTHQ10.

for 60 min after the startup shear flow in PSHQ10, PTHQ10, and PEHQ10 at $T_{NI} - 40$ °C for $\dot\gamma = 0.6\ s^{-1}$. Figure 7 describes (i) variations of $N_1^+(t,\dot\gamma)$ upon startup shear flow, (ii) variations of first normal stress difference decay $N_1^-(t,\dot\gamma)$ upon cessation of steady-state shear flow, and (iii) variations of $N_1^+(t,\dot\gamma)$ in intermittent shear flow followed by a long rest for 60 min after the startup shear flow in PSHQ10, PTHQ10, and PEHQ10 at $T_{NI} - 40$ °C for $\dot\gamma = 0.6\ s^{-1}$. Notice in Figures 6 and 7 that startup and intermittent shear flow experiments were conducted at $T_{NI} - 40$ °C, the same distance below the T_{NI} of the respective polymers, to compare the rheological responses of the three TLCPs without the effect of molecular weight.

Figure 8 compares normalized shear stress decay $\sigma^-(t,\dot\gamma)/\sigma_0$ and normalized first normal stress difference decay $N_1^-(t,\dot\gamma)/N_{1,0}$ of PSHQ10, PEHQ10, and PTHQ10 upon cessation of steady-state shear flow, where σ_0 denotes the steady-state shear stress at $\dot\gamma = 0.6\ s^{-1}$ and $N_{1,0}$ denotes the steady-state first normal stress difference at $\dot\gamma = 0.6\ s^{-1}$. In Figure 8 we observe that among the three TLCPs under investigation the relaxation of both $\sigma^-(t,\dot\gamma)/\sigma_0$ and $N_1^-(t,\dot\gamma)/N_{1,0}$ is slowest with PSHQ10 and is fastest with PTHQ10. This observation again seems to reflect the bulkiness of pendent side groups in each TLCP investigated; i.e., PSHQ10 with phenylsulfonyl pendent side groups exhibits the slowest rate of stress decay, while PTHQ10 exhibits the fastest rate of stress decay. Again, we believe that the choice of a temperature that is at the same distance below the T_{NI} of the respective TLCPs has enabled us to make a fair comparison describing the effect of the bulkiness of pendent side groups on the stress relaxation behavior of the three TLCPs investigated.

After cessation of steady-state shear flow followed by a rest for 1 h, the same specimen was subjected to another transient shear flow (often referred to as intermittent shear flow). Variations of $\sigma^+(t,\dot\gamma)$ with time during intermittent shear flow are given on the inset of the right side of Figure 6, and variations of $N_1^+(t,\dot\gamma)$ with time during intermittent shear flow are given on the inset of the right side of Figure 7, for PSHQ10, PTHQ10, and PEHQ10 at $T_{NI} - 40$ °C and at $\dot\gamma = 0.6\ s^{-1}$. The purpose of the experiment was to investigate the effect of previous deformation history followed by stress relaxation on intermittent shear flow. Such an experiment is particularly interesting for TLCP because

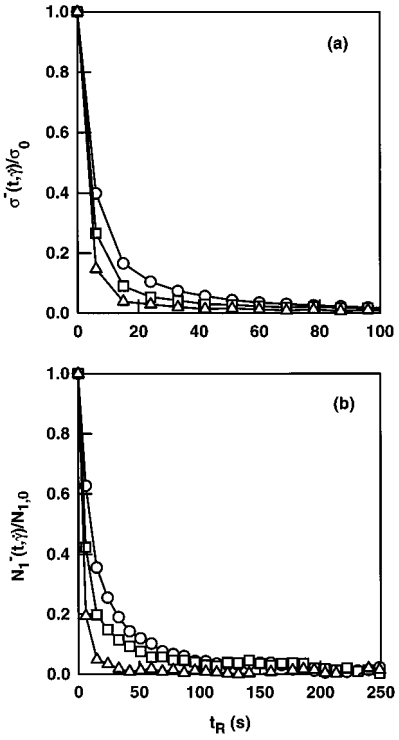

Figure 8. Plots of (a) shear stress decay $\sigma^-(t,\dot\gamma)$ versus $\dot\gamma t$ and (b) first normal stress difference decay $N_1^-(t,\dot\gamma)$ versus $\dot\gamma t$, upon cessation of steady-state shear flow at $\dot\gamma = 0.6$ s^{-1} and at $T_{NI} - 40$ °C in the nematic region for (○) PSHQ10, (□) PEHQ10, and (△) PTHQ10.

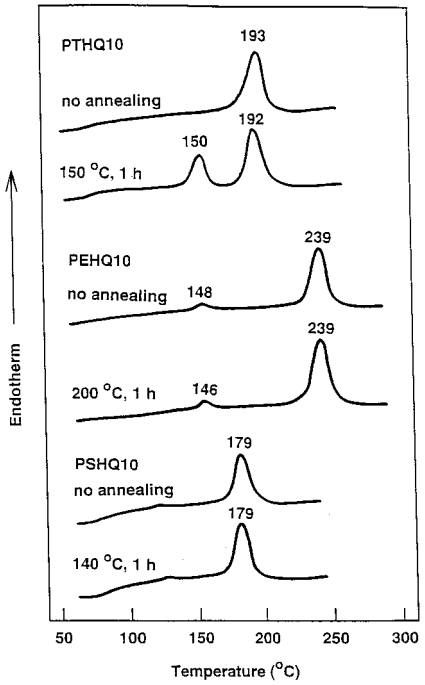

Figure 9. DSC traces before and after annealing of PTHQ10, PEHQ10, and PSHQ10. The annealing conditions employed are given on the DSC trace. Notice that a new endothermic peak appears at 150 °C for PTHQ10 after annealing for 1 h, whereas no such endothermic peak appears for PEHQ10 and PSHQ10.

often the mesophase texture in TLCP recovers with time during rest after cessation of shear flow.

In Figures 6 and 7 we observe that the peak values of $\sigma^+(t,\dot\gamma)$ and $N_1^+(t,\dot\gamma)$ during intermittent shear flow are the largest in PSHQ10 among the three TLCPs under investigation. The readers are reminded that the same trend was observed during startup shear flow (Figure 4). It is interesting to note in Figure 7 that the peak value of $N_1^+(t,\dot\gamma)$ during intermittent shear flow is larger in PTHQ10 than in PEHQ10. This trend, however, is opposite to that observed in startup shear flow (Figure 4). To explain the seemingly peculiar rheological response of $N_1^+(t,\dot\gamma)$ observed in PTHQ10 during intermittent shear flow, using DSC we investigated whether there might have been a significant change in morphology in each of the three TLCPs investigated. Figure 9 gives DSC traces of as-cast specimens of the three TLCPs under investigation, each of which having been annealed in a vacuum oven for varying periods at a preset temperature: (i) PTHQ10 at 150 °C, (ii) PSHQ10 at 140 °C, and (iii) PEHQ10 at 200 °C. The annealing temperatures of these polymers were chosen such that they could be at the same distance below the T_{NI} of the respective polymers, $T_{NI} - 40$ °C. Interestingly, in Figure 9 we observe the growth of the lower endothermic peak in PTHQ10, which is attributable to the formation of high-temperature melting crystals via crystallization during annealing,[7] but not in PEHQ10 and PSHQ10. We can thus conclude that the larger peak value of $N_1^+(t,\dot\gamma)$ in PTHQ10, compared to the peak value of $N_1^+(t,\dot\gamma)$ in PEHQ10, observed in Figure 7, is due to the formation and growth of high-temperature melting crystals that were formed during the rest period of 60 min after cessation of steady shear flow.

Another interesting observation that can be made in Figure 6 is that the peak values of $\sigma^+(t,\dot\gamma)$ in intermittent shear flow of all three TLCPs are much smaller than those observed in startup shear flow. Specifically, in Figure 6 we observe that the peak value of $\sigma^+(t,\dot\gamma)$ for PTHQ10 in intermittent shear flow is about 25% of that in startup shear flow, the peak value of $\sigma^+(t,\dot\gamma)$ for PEHQ10 is about 15% of that in startup shear flow, and the peak value of $\sigma^+(t,\dot\gamma)$ for PSHQ10 in intermittent shear flow is about 10% of that in startup shear flow. What is most interesting in Figure 7 is that the peak value of $N_1^+(t,\dot\gamma)$ for PTHQ10 in intermittent shear flow is even greater than that in startup shear flow, whereas the peak value of $N_1^+(t,\dot\gamma)$ for PEHQ10 in intermittent shear flow is comparable to that in startup shear flow and the peak value of $N_1^+(t,\dot\gamma)$ for PSHQ10 in intermittent shear flow is one-half of that in startup shear flow. The larger peak value of $N_1^+(t,\dot\gamma)$ in PTHQ10 during intermittent shear flow, compared to the peak value of $N_1^+(t,\dot\gamma)$ during startup shear flow, is again attributable to the formation and growth of high-temperature melting crystals in PTHQ10 that were formed during the rest period of 60 min after cessation of steady shear flow (Figure 9). Since the same observation is not made for the peak value of $\sigma^+(t,\dot\gamma)$ for PTHQ10, it is fair to state that $N_1^+(t,\dot\gamma)$ is much more sensitive to a variation in morphology of specimen than $\sigma^+(t,\dot\gamma)$.

3.3. Time Evolution of Dynamic Moduli after Cessation of Steady Shear Flow. On the basis of the observations made above on the rheological responses in intermittent shear flow, we thought that it would be interesting to investigate variations of dynamic moduli (G' and G'') with time after cessation of shear flow. For this, a specimen was subjected to steady shear flow at a given $\dot\gamma$, and upon cessation of steady shear flow, the time evolution of G' and G'' of the specimen was monitored for a long period by applying intermittently a very small amplitude (0.02) oscillatory shear motion at an angular frequency of 0.1 rad/s. Figure 10a gives

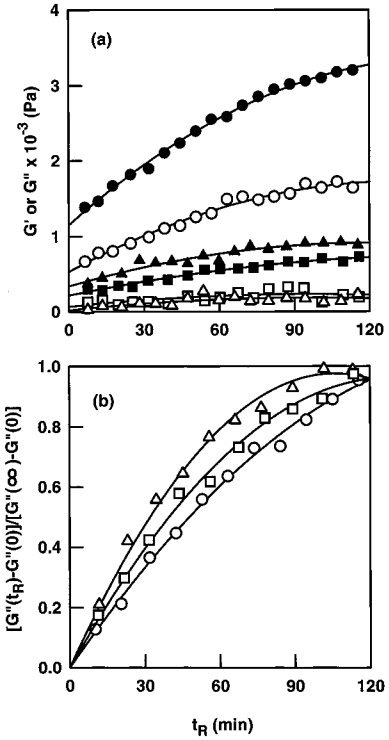

Figure 10. (a) Variations of dynamic storage modulus G' (open symbols) and dynamic loss modulus G'' (filled symbols) with rest time (t_R) after cessation of steady shear flow at $\dot{\gamma} = 0.6\ s^{-1}$ and at $T_{NI} - 40$ °C in the nematic region for (○, ●) PSHQ10, (□, ■) PEHQ10, and (△, ▲) PTHQ10. (b) Variations of reduced dynamic loss modulus $[G''(t_R) - G''(0)]/[G''(\infty) - G''(0)]$ with t_R after cessation of steady-state shear flow at $\dot{\gamma} = 0.6\ s^{-1}$ and at $T_{NI} - 40$ °C in the nematic region for (○) PSHQ10, (□) PEHQ10, and (△) PTHQ10. The strain amplitude of 0.02 and angular frequency of 0.1 rad/s were used, which were well within the linear viscoelastic range of the polymers investigated.

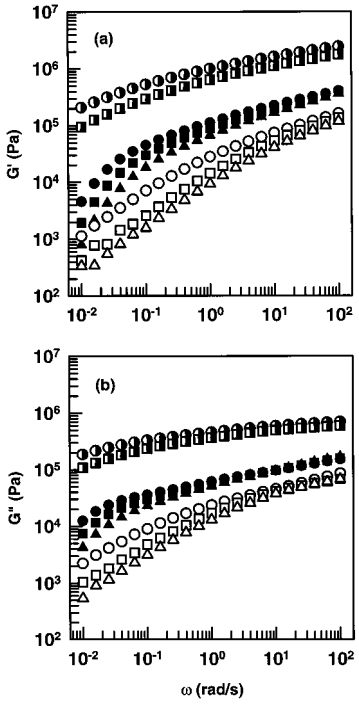

Figure 11. Plots of (a) log G' versus log ω and (b) log G'' versus log ω for PEHQ10. In the smectic region at various temperatures: (◑) 130 °C and (◨) 135 °C. In the nematic region at various temperatures: (○) 160 °C, (□) 200 °C, and (△) 210 °C. In the isotropic region: (●) 250 °C, (■) 255 °C, and (▲) 260 °C.

variations of G' and G'' with rest time (t_R) for PSHQ10, PTHQ10, and PEHQ10 after cessation of steady-state shear flow at $T_{NI} - 40$ °C and $\dot{\gamma} = 0.6\ s^{-1}$. It can be seen in Figure 10a that values of G' are much smaller than those of G'' throughout the entire rest period investigated and that initially both G' and G'' increase with t and then level off at a later time. Similar results were obtained for different values of $\dot{\gamma}$.

Figure 10b describes variations of reduced dynamic loss modulus G''_R with rest time t_R where $G''_R = [G''(t_R) - G''(0)]/[G''(\infty) - G''(0)]$ with $G''(0)$ being the initial value of dynamic loss modulus after cessation of shear flow and $G''(\infty)$ being the dynamic loss modulus after a sufficiently long rest time.[29] From the slope of the curves in Figure 10b we can conclude that the increasing rate of G''_R takes place at the slowest rate for PSHQ10 and at the fastest rate for PTHQ10 among the three TLCPs under investigation. The observed difference in the increasing rate of G''_R between PSHQ10 and PTHQ10 can be explained by an observation that the mobility of PSHQ10 with pendent side groups having the largest van der Waals volume among the three different pendent side groups under consideration would be much less than the mobility of PTHQ10.

3.4. Oscillatory Shear Flow Behavior. Figure 11 gives log G' versus log ω and log G'' versus log ω plots for PEHQ10 (i) at 135 °C in the smectic region, (ii) at 160, 200, and 210 °C in the nematic region, and (iii) at 250, 255, and 260 °C in the isotropic region. The following observations are worth noting in Figure 11. Values of G' and G'' in the smectic region are much greater than those in the nematic region, which is not surprising in that the smectic phase has 2-dimensional textures while the nematic phase has 1-dimensional textures. This finding is in agreement with the previous studies by Hudson et al.,[16] who also used PEHQ10, and by Rubin et al.,[30] who used side-chain TLCPs having methacrylate backbone, six methylene units as flexible spacer, and phenyl benzoate mesogens. In reference to Figure 11, values of G' and G'' at 160, 200, and 210 °C in the nematic region are lower than those at 250, 255, and 260 °C in the isotropic region, behavior also reported by previous investigators.[16,30]

The seemingly peculiar dynamic viscoelastic behavior observed in Figure 11 is characteristic of TLCP, which is attributable to a change in the orientational order parameter of the nematic phase with temperature. This can best be illustrated by the plots of steady-state shear viscosity η versus temperature, given in Figure 12, for PEHQ10, PSHQ10, and PTHQ10. In reference to Figure 12, η of PEHQ10 (i) drops precipitously at about 148 °C (close to T_{SN}), (ii) decreases steadily with increasing temperature to about 200 °C, (iii) increases rapidly with increasing temperature to about 240 °C (close to T_{NI}), and (iv) decreases slowly with increasing the temperature further. A similar observation can be made in Figure 12 for PTHQ10 and PSHQ10. As a matter of fact, such an observation was reported previously.[31,32] A decrease of η for PEHQ10 with increasing temperature to about 200 °C is attributable to the orientation of an anisotropic phase along the shear direction, and an increase of η with increasing temperature to about 240 °C is attributable to the existence of a biphasic region that is due to the polydisperse nature of the polymer; i.e., the low-molecular-weight portion of the polymer

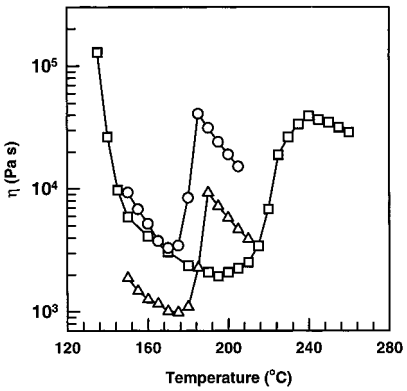

Figure 12. Temperature dependence of steady-state shear viscosity η at $\dot{\gamma} = 0.3\ s^{-1}$ for (○) PSHQ10, (□) PEHQ10, and (△) PTHQ10.

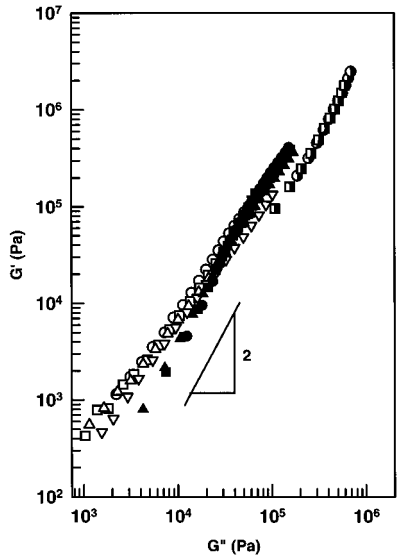

Figure 13. Han plots for PEHQ10. In the smectic region at various temperatures: (◑) 130 °C and (◨) 135 °C. In the nematic region at various temperatures: (○) 160 °C, (□) 200 °C, (△) 210 °C, and (▽) 230 °C. In the isotropic region: (●) 250 °C, (■) 255 °C, and (▲) 260 °C.

begins to transform into an isotropic region at temperatures below T_{NI}. In reference to Figure 12, a decrease of η with increasing temperature in the isotropic region (i.e., above T_{NI}) can be explained by an Arrhenius relationship. Notice in Figure 12 that η in the smectic region (at 130 and 135 °C) of PEHQ10 is exceedingly high, which is attributable to the presence of 2-dimensional textures.

Figure 13 gives log G' versus log G'' plots for PEHQ10 at various temperatures in smectic, nematic, and isotropic regions, which were prepared from Figure 11. Following Neumann et al.,[33] hereafter log G' versus log G'' plot will be referred to as the Han plot. It should be pointed out that the Han plot has *no* relation whatsoever with the empirical Cole−Cole plot,[34] which gives a *temperature-dependent* semicircle in *rectangular* coordinates, and that the Han plot has as its basis a molecular viscoelasticity theory.[35] There are three significant features that deserve an elaboration in Figure 13: (i) the Han plot in the nematic region has a slope less than 2 in the terminal region and shows a very weak temperature dependence at temperatures below 210 °C; (2) the Han plot moves downward as the temperature is increased to 210 °C still in the nematic region having a slope less than 2 in the terminal region;

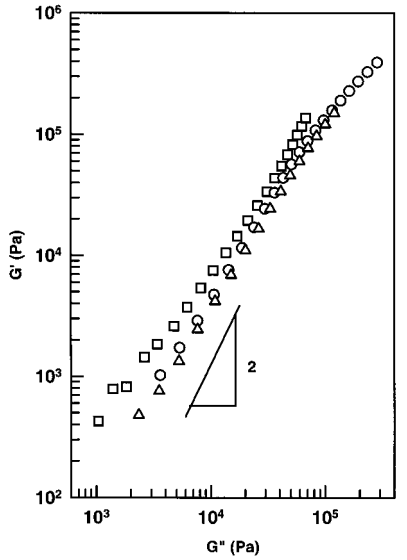

Figure 14. Han plots at $T_{NI} - 40$ °C in the nematic region for (○) PSHQ10, (□) PEHQ10, and (△) PTHQ10.

and (iii) the Han plot exhibits temperature independence at 250, 255, and 260 °C in the isotropic region. Similar observations were made, not presented here, for PTHQ10 and PSHQ10. According to Han et al.,[35] the Han plot is expected to have a slope of 2 in the terminal region and is virtually independent of temperature for all homopolymers and other types of polymers in the isotropic state, and moreover, the Han plot is expected to be independent of molecular weight for entangled polymers. It should be mentioned that the Han plot has successfully been used to determine the order−disorder transition temperature of block copolymers.[36,37] We can conclude from Figure 13 that the Han plot is very effective to determine the T_{NI} of TLCP. We wish to emphasize that Han plot, however, cannot determine the mesophase structure present in a TLCP; i.e., the Han plot should not be regarded as being a tool for determining phase morphology.

In the past, plots of log G' versus log ω and log G'' versus log ω have been used successfully to obtain so-called master (or reduced) plots by shifting the data obtained at different temperatures to a set of data obtained at a particular temperature chosen as reference state, a procedure commonly referred to as time−temperature superposition (TTS). It should be mentioned that TTS presumes that the morphological state of a polymer remains *unchanged* over the entire range of temperatures where TTS is applied. This now brings us to a very fundamental question: Can we justify the application of TTS to TLCPs in an anisotropic state whose morphological state varies with temperature? Having seen the temperature dependence of Han plots given in Figure 13, we believe that use of TTS is not warranted to obtain reduced plots for TLCPs in an anisotropic state as long as the Han plot shows a temperature dependence.

Figure 14 gives Han plots for PEHQ10, PTHQ10, and PSHQ10 at $T_{NI} - 40$ °C in the nematic region. Notice in Figure 13 that the Han plot depended on temperature in an anisotropic region. In view of the fact that the three TLCPs under consideration have different values of T_{NI}, for comparison we have chosen $T_{NI} - 40$ °C, so that each polymer is at the same distance below its T_{NI}. It can be seen in Figure 14 that the ratio G'/G'' is ranked as follows: G'/G'' for PEHQ10 > G'/G'' for PSHQ10 >

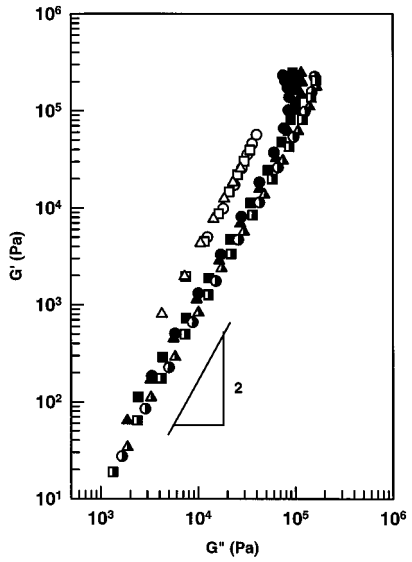

Figure 15. Han plots in the isotropic region. PEHQ10 at various temperatures: (○) 250 °C, (□) 255 °C, and (△) 260 °C. PSHQ10 at various temperatures: (●)185 °C, (■) 190 °C, and (▲) 195 °C. PTHQ10 at various temperatures: (◑) 195 °C, (◨) 200 °C, and (◭) 205 °C.

G'/G'' for PTHQ10. Figure 15 gives Han plots for PEHQ10, PTHQ10, and PSHQ10 at various temperatures in the isotropic region. It can be seen in Figure 15 that the ranking of the ratio G'/G'' in the isotropic region is the same as that in the nematic state of the three TLCPs investigated. To ascertain whether we can draw the same conclusion from steady-state shear flow experiment, from Figure 4 we calculated the ratio N_1/σ and obtained the following results: $N_1/\sigma = 13.48$ at $\sigma = 780$ Pa for PEHQ10, $N_1/\sigma = 10.02$ at $\sigma = 4720$ Pa for PSHQ10, and $N_1/\sigma = 5.83$ at $\sigma = 640$ Pa for PTHQ10. In view of the fact that Han plot is expected to be independent of molecular weight for entangled polymers, the observations made from Figures 14 and 15 may be attributable to the differences in chemical structure of the pendent side groups under consideration, provided that all three TLCPs are in the entangled regime. However, at present we have no information on the entanglement molecular weight of the three polymers.

Figure 16a gives log $|\eta^*|$ versus log ω plots for PEHQ10, PTHQ10, and PSHQ10 at $T_{NI} + 15$ °C in the isotropic region, where $|\eta^*|$ is complex viscosity. It can be seen in Figure 16a that PEHQ10 is the most viscous and PTHQ10 is the least viscous in the isotropic region. In the isotropic state of TLCP (or any homopolymers), both temperature and molecular weight (and molecular weight distribution) would affect melt viscosity. To suppress the effect of temperature on the viscosity of the three TLCPs in the isotropic state, in Figure 16 we compare values of $|\eta^*|$ for the three TLCPs at $T_{NI} + 15$ °C, the same distance below the T_{NI} of the respective TLCPs. We are not aware of any parameter that might be used to suppress or eliminate the effect of molecular weight on the viscosity of TLCPs in the isotropic region. In view of the fact that, among the three TLCPs under consideration, PEHQ10 has very high intrinsic viscosity compared to that of PTHQ10 and PSHQ10 (Table 1), it is very reasonable to speculate that the molecular weight of PEHQ10 is much higher than that of PTHQ10 and PSHQ10. Notice in Table 1 that the intrinsic viscosity of PSHQ10 is slightly lower than that of

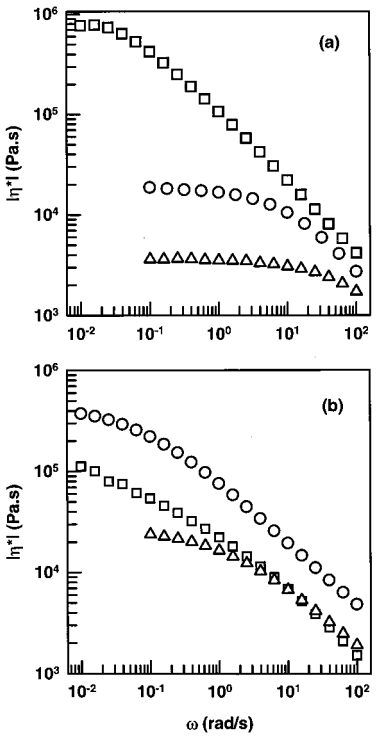

Figure 16. (a) Plots of log $|\eta^*|$ versus log ω at $T_{NI} + 15$ °C in the isotropic region for (□) PEHQ10, (○) PSHQ10, and (△) PTHQ10. (b) Plots of log $|\eta^*|$ versus log ω at $T_{NI} - 40$ °C in the nematic region for (○) PSHQ10, (□) PEHQ10, and (△) PTHQ10.

PTHQ10. And yet, in Figure 16a we observe that PSHQ10 has higher $|\eta^*|$ than that of PTHQ10, suggesting to us that the bulkiness of phenylsulfonyl pendent side groups in PSHQ10 must have played a predominant role over the difference in molecular weight between PSHQ10 and PTHQ10 in determining $|\eta^*|$. On the other hand, when the difference in molecular weight between two TLCPs is very large, like the situation between PEHQ10 and PTHQ10, the difference in molecular weight might outweigh the difference in bulkiness between the two TLCPs in determining the viscosities of the TLCPs. We thus speculate that the difference in molecular weight between PEHQ10 and PTHQ10, and between PEHQ10 and PSHQ10, might have outweighed the difference in bulkiness between the two TLCPs, giving rise to much higher values of $|\eta^*|$ for PEHQ10, compared to the value of $|\eta^*|$ for PTHQ10 and PSHQ10, in the isotropic region. Note that in the isotropic region the molecules of the TLCPs under consideration would lose all ordered structures, and thus they can be regarded as being semiflexible macromolecular chains having no preferential orientation in any particular direction during shear flow.

The situation will become quite different when the same TLCPs are subjected to shear flow in the *nematic* state, because the molecules in the nematic state would exhibit preferential orientation during shear flow. Figure 16b gives log $|\eta^*|$ versus log ω plots for PEHQ10, PTHQ10, and PSHQ10 at $T_{NI} - 40$ °C in the nematic region. In Figure 16b we observe that among the three TLCPs under consideration PSHQ10 is the most viscous and PTHQ10 is the least viscous in the nematic region. If we postulate that the bulkier pendent phenylsulfonyl side groups would have a greater difficulty to orient under shear flow, compared to less bulky ethoxy or *tert*-butyl pendent side groups, we can then explain why

PSHQ10 is more viscous than PTHQ10 and PEHQ10 in the nematic region. Thus, in the nematic region the bulkiness of pendent side groups in TLCP is expected to play a much greater role compared to the difference in molecular weight between two TLCPs. This observation seems to explain why in Figure 16b the values of $|\eta^*|$ of PSHQ10 having phenylsulfonyl pendent side groups, which are much bulkier than the ethoxy pendent side groups in PEHQ10, are much greater than those of PEHQ10, although the molecular weight of PEHQ10 is believed to be much higher than that of PSHQ10.

4. Concluding Remarks

In this paper we have shown how the bulkiness of pendent side groups affects the rheological behavior of TLCPs. We found that, among the three TLCPs investigated, PSHQ10 having the largest van der Waals volume has (i) the largest peak value of $\sigma^+(t,\dot{\gamma})$ and $N_1^+(t,\dot{\gamma})$ during startup shear flow, (ii) the slowest rate of stress relaxation upon cessation of steady-state shear flow, and (iii) the slowest rate of G''_R increase after a long rest upon cessation of steady-state shear flow. We have shown that comparison of the rheological properties in the nematic region of TLCPs having different values of T_{NI} can be made at a temperature that is at the same distance below the clearing temperature of the respective polymers. We have shown from the Han plot that application of TTS to TLCPs in an anisotropic region is not warranted.

At present there exists no theory predicting the rheological behavior of semiflexible TLCPs investigated in this study. In view of the fact that the clearing temperature of TLCPs without flexible spacers (i.e., rigid-rod-like TLCPs) is very high in general, giving rise to practical difficulties with processing, it is essential for one to include the flexibility of TLCP chains in future development of theory, which will enable us to predict the rheological behavior of semiflexible TLCPs. To develop such theory, one must first have an accurate expression for an excluded-volume potential for semiflexible polymer chains. An intermolecular potential of the Maier−Saupe form, which was developed for low-molecular-weight nematics, is not adequate to describe the dynamics and rheological behavior of semiflexible polymer chains. This is one of the many areas that require a greater attention of polymer scientists if there is going to be a meaningful progress on a better understanding of the dynamics and rheological behavior of TLCPs.

In this paper we have shown that the bulkiness of pendent side groups also plays a significant role in determining the rheological behavior of TLCPs in an anisotropic state. Specifically, variations of the chemical structure of pendent side groups would greatly influence the dynamics and rheological behavior, hence processability, of TLCPs. Therefore, in future development of theory, it is very important to include pendent side groups in semiflexible TLCP. On the other hand, there are relatively few experimental studies reported in the literature that can be used for future development of theory. As pointed out above, rheological measurements of TLCPs must be conducted in such a way that they can be reproducible. This can only be realized when initial conditions of specimens are reproducible, which in turn can be realized when using TLCPs having a clearing temperature below thermal degradation temperature. Therefore, more systematic experimental investigations on the dynamics and rheological behavior of semiflexible TLCPs are needed to establish a firm scientific basis on which meaningful theory can be developed. We found that the bulkiness of pendent side groups greatly influences the rheological behavior of the TLCPs synthesized in this study.

Acknowledgment. We acknowledge that this study was supported in part by the National Science Foundation under Grant CTS-9614929.

References and Notes

(1) Cocchini, F.; Nobile, M. R.; Acierno, D. *J. Rheol.* **1991**, *35*, 1171.
(2) Guskey, S. M.; Winter, H. H. *J. Rheol.* **1991**, *35*, 1191.
(3) Han, C. D.; Chang, S.; Kim, S. S. *Mol. Cryst. Liq. Cryst.* **1994**, *254*, 335.
(4) Kim, S. S.; Han, C. D. *Macromolecules* **1993**, *26*, 3176.
(5) Kim, S. S.; Han, C. D. *Polymer* **1994**, *35*, 93.
(6) Cocchini, F.; Nobile, M. R.; Acierno, D. *J. Rheol.* **1992**, *36*, 13.
(7) Han, C. D.; Chang, S.; Kim, S. S. *Macromolecules* **1994**, *27*, 7699.
(8) Chang, S.; Han, C. D. *Macromolecules* **1997**, *30*, 1656.
(9) Kim, S. S.; Han, C. D. *Macromolecules* **1993**, *26*, 6633.
(10) Kim, S. S.; Han, C. D. *J. Rheol.* **1993**, *37*, 847; **1994**, *38*, 13.
(11) Chang, S.; Han, C. D. *Macromolecules* **1997**, *30*, 2021.
(12) Furukawa, A.; Lenz, R. W. *Macromol. Chem., Macromol. Symp.* **1986**, *2*, 3.
(13) Lenz, R. W.; Furukawa, A.; Bhowmik, P. K.; Garay, R. O.; Majnusz, J. *Polymer* **1991**, *32*, 1703.
(14) Chang, S.; Han, C. D. *Macromolecules* **1997**, *30*, 1670.
(15) Kim, D.-O.; Han, C. D. Manuscript in preparation.
(16) Hudson, S. D.; Lovinger, A. J.; Larson, R. G.; Davis, D. D.; Garay, R. O.; Fujihiro, K. *Macromolecules* **1993**, *26*, 5643.
(17) Marrucci, G.; Maffettone, P. L. *J. Rheol.* **1991**, *34*, 1217, 1231.
(18) Maier, W.; Saupe, A. *Z. Naturforch.* **1958**, *13A*, 564; **1959**, *14A*, 882; **1960**, *15A*, 287.
(19) Blumstein, A.; Vilasagar, S.; Ponrathnam, S.; Clough, S. B.; Blumstein, R. B.; Maret, G. *J. Polym. Sci., Polym. Phys. Ed.* **1982**, *20*, 877.
(20) Majnusz, J.; Catala, J. M.; Lenz, R. W. *Eur. Polym. J.* **1983**, *19*, 1043.
(21) Blumstein, R. B.; Stickles, E. M.; Gautheir, M. M.; Blumstein, A.; Volino, F. *Macromolecules* **1984**, *17*, 177.
(22) Percec, V.; Tomazos, D.; Pugh, C. *Macromolecules* **1989**, *22*, 3259.
(23) Laus, M.; Sante Angeloni, A.; Galli, G.; Chiellini, E. *Macromolecules* **1992**, *25*, 5901.
(24) Baek, S. G.; Magda, J.; Larson, R. G.; Hudson, S. D. *J. Rheol.* **1994**, *38*, 1473.
(25) Kiss, G.; Porter, R. S. *J. Polym. Sci., Polym. Symp.* **1978**, *65*, 193.
(26) Kiss, G.; Porter, R. S. *J. Polym. Sci., Polym. Phys.* **1980**, *18*, 361.
(27) Navard, P.; Haudin, J. M. *J. Polym. Sci., Polym. Phys.* **1986**, *24*, 189.
(28) Baek. S. G.; Magda, J.; Larson, R. G.; Hudson, S. D. *J. Rheol.* **1993**, *37*, 1201.
(29) Grizzuti, N.; Moldenaers, P.; Mortier, M.; Mewis, J. *Rheol. Acta* **1993**, *32*, 218.
(30) Rubin, S. F.; Kannan, R. M.; Kornfield, J. A.; Boeffel, C. *Macromolecules* **1995**, *28*, 3521.
(31) Wunder, S. L.; Ramachandran, S.; Cochanour, C. R.; Weinberg, M. *Macromolecules* **1986**, *19*, 9, 1696.
(32) Kim, S. S.; Han, C. D. *J. Polym. Sci., Part B: Polym. Phys.* **1994**, *32*, 371.
(33) Neumann, C.; Loveday, D. R.; Abetz, V.; Stadler, R. *Macromolecules* **1998**, *31*, 2493. These authors referred to the log G' versus log G'' plot as the Han plot.
(34) Cole, K. S.; Cole, R. H. *J. Chem. Phys.* **1941**, *9*, 341.
(35) (a) Han, C. D.; Jhon, M. S. *J. Appl. Polym. Sci.* **1986**, *32*, 3809. (b) Han, C. D.; Kim, J. K. *Macromolecules* **1989**, *22*, 4292.
(36) (a) Han, C. D.; Kim, J. *J. Polym. Sci., Polym. Phys. Ed.* **1987**, *25*, 1741. (b) Han, C. D.; Kim, J.; Kim, J. K. *Macromolecules* **1989**, *22*, 383. (c) Han, C. D.; Baek, D. M.; Kim, J. K. *Macromolecules* **1990**, *23*, 561.
(37) Han, C. D.; Baek, D. M.; Kim, J. K.; Ogawa, T.; Sakamoto, N.; Hashimoto, T. M*acromolecules* **1995**, *28*, 5043.

MA9915879